ORIGINAL ARTICLE

ACTA RADIOLOGICA

Physical and Clinical Comparison between a Screen-Film System and a Dual-Side Reading Mammography-Dedicated Computed Radiography System

S. Rivetti[1], B. Canossi[2], R. Battista[2], N. Lanconelli[3], E. Vetruccio[2], C. Danielli[4], G. Borasi[5] & P. Torricelli[2]

[1]Department of Health Physics, AUSL Modena, Modena, Italy; [2]Department of Radiology, University of Modena and Reggio Emilia, Modena, Italy; [3]Department of Physics, University of Bologna, Bologna, Italy; [4]Department of Health Physics, Policlinico di Modena, Modena, Italy; [5]Department of Health Physics, Arcispedale Santa Maria Nuova, Reggio Emilia, Italy

Rivetti S, Canossi B, Battista R, Lanconelli N, Vetruccio E, Danielli C, Borasi G, Torricelli P. Physical and clinical comparison between a screen-film system and a dual-side reading mammography-dedicated computed radiography system. Acta Radiol 2009;50:1109–1118.

Background: Digital mammography systems, thanks to a physical performance better than conventional screen-film units, have the potential of reducing the dose to patients, without decreasing the diagnostic accuracy.

Purpose: To achieve a physical and clinical comparison between two systems: a screen-film plate and a dual-side computed radiography system (CRM; FUJIFILM FCR 5000 MA).

Material and Methods: A unique feature of the FCR 5000 MA system is that it has a clear support medium, allowing light emitted during the scanning process to be detected on the "back" of the storage phosphor plate, considerably improving the system's efficiency. The system's physical performance was tested by means of a quantitative analysis, with calculation of the modulation transfer function, detective quantum efficiency, and contrast-detail analysis; subsequently, the results were compared with those achieved using a screen-film system (SFM; Eastmann Kodak MinR-MinR 2000). A receiver operating characteristic (ROC) analysis was then performed on 120 paired clinical images obtained in a craniocaudal projection with the conventional SFM system under standard exposure conditions and also with the CRM system working with a dose reduced by 35% (average breast thickness: 4.3 cm; mean glandular dose: 1.45 mGy). CRM clinical images were interpreted both in hard copy and in soft copy.

Results: The ROC analysis revealed that the performances of the two systems (SFM and CRM with reduced dose) were similar ($P>0.05$): the diagnostic accuracy of the two systems, when valued in terms of the area underneath the ROC curve, was found to be 0.74 for the SFM, 0.78 for the CRM (hard copy), and 0.79 for the CRM (soft copy).

Conclusion: The outcome obtained from our experiments shows that the use of the dual-side CRM system is a very good alternative to the screen-film system.

Key words: Breast radiography, comparative studies, digital mammography, dose reduction

Nico Lanconelli, Dipartimento di Fisica, Viale Berti-Pichat 6/2, I-40127 Bologna BO, Italy (tel. +39 051 2095136, fax. +39 051 2095047, e-mail. nico.lanconelli@unibo.it)

Accepted for publication July 10, 2009

Mammography is the most widely used technique for the diagnosis of breast cancer. The use of digital mammography systems, as an alternative to the conventional screen-film technique, has become current practice (1–3). The main advantages of digital systems lie above all in the capability for individual optimization of the acquisition, recording, and display of images. Further, digital processing of images (picture archiving, communications systems, and teleconsulting systems) is allowed with digital systems. Since these systems are becoming widespread, it is particularly important to investigate their optimal working conditions, in order to maximize their performance in terms of doses administered and quality of diagnosis.

Digital systems are intrinsically more suitable for quantitative characterization than screen-film equivalents, and since their images have a numerical structure, they can be studied more effectively through the application of relatively simple, repeatable procedures. This has encouraged interest in comparative analysis studies

informa
healthcare

DOI 10.3109/02841850903271333

aiming to assess the technologies available and optimize the phases of the image formation processes, in order to develop methods that maximize diagnostic content while reducing the radiation doses received by patients (4).

In this paper, we first present a comparison of a mammography-dedicated dual-side reading computed radiography (CRM) system with a conventional screen-film system (SFM), still the most widespread and gold-standard system in mammography practice. The initial comparison was done at about the same dose. After that, a further comparison between the same CRM images used in the previous case and CRM images acquired at a reduced dose was conducted.

Material and Methods

The physical performance levels of the SFM and CRM systems were assessed through quantitative analysis using physical characterization (A) and contrast-detail analysis (B). Subsequently, a receiver operating characteristic (ROC) analysis (C) was performed on a set of pairs of clinical images from a craniocaudal view, obtained first with conventional SFM under standard exposure conditions, and thereafter with a CRM with a dose reduced by 35%.

Two systems were considered, the first being the mammography-dedicated FCR 5000 MA Plus CRM unit (FUJIFILM Corporation, Tokyo, Japan). A unique feature of this system is that the storage phosphor ($BaF(Br,I)Eu^{2+}$, pixel size: 50 μm) has a transparent support and a reading device that can detect emissions from both sides of the image plate to improve image quality (5). This system has been approved in the U.S. for full-field digital mammography application.

For physical characterization and phantom analysis, the postprocessing was done with FIX-MODE screen processing, with parameters S=139 (sensitivity) and L=2 (latitude). The response curve of the CRM system was determined by exposing the detector to a wide range of uniform X-ray exposures. Due to the logarithmic response of the system, all the image data used for the physical measurements were linearized by means of the fitted-response function. The digital images from the CRM unit were also printed by a FUJIFILM DPL laser printer (pixel size: 50 μm) and displayed on a dedicated monitor (EIZO FC-2090, 2048×1536 pixels, 8 bit, max. luminance 650 cd/m2; EIZO Nanao Corporation, Hakusan, Japan).

The second system considered was a MinR-MinR 2000 SFM system (Eastman Kodak Company, Rochester, N.Y., USA). The X-ray source used throughout the study was a "Sophie" mammography unit (Planmed, Helsinki, Finland). A mammography-dedicated Kodak Min-loader Day-Light attached to a MinR processor (120 s, 35.0°C) was used (Kodak Wratten; Eastman Kodak Company, Rochester, N.Y., USA). The clinical mammography unit and the CR receptor used underwent all regular quality assurance checks, according to the European Reference Organisation for Quality Assured Breast Screening and Diagnostic Services (EUREF) guidelines. In particular, measurements concerning the radiographic generation unit, the image receptor, the image quality, and the image presentation were performed with the procedures and the frequency suggested by the guidelines. The automatic exposure control (AEC) of the mammography unit was calibrated for the film-screen cassettes. The same setup was used for the CR system, except for changing the exposure time, when the "low dose" condition is needed.

During the clinical trial, 120 women were enrolled, as part of the conventional study, by means of a dual exposure of the same breast obtained in a craniocaudal view with the conventional SFM under standard exposure conditions and the CRM working with a 35% reduction in dose, as in the contrast-detail analysis. The pairs of images were acquired in sequence without removing the compression paddle. Each woman signed an informed consent form approved by the institutional review board, and the investigation was approved by the ethics committee of the hospital. Four experienced radiologists independently assigned a Breast Imaging Reporting and Data System (BI-RADS) category to the SFM and CRM images using the range R1–R5. The gold standard for cases classified as R4 and R5 was histological examination, while for the others mammographic biennial follow-up was used. The set of images used consisted of 34 images classified in the range R3–R5 by the radiologist panel, and 86 images classified as R1 or R2. Most of the images contained masses, microcalcifications, or architectural distortions. Specifically, 39 masses (27 without calcifications, four with calcifications, six lymph nodes, and two oil cysts), 62 calcifications (29 surgical, 19 spread, seven clusters, and seven vascular), and 46 architectural distortions (43 surgical and three radial scars) were considered.

Physical characterization

The image quality of the two systems, their spatial resolution, and their efficiency were evaluated by calculating the modulation transfer function (MTF) and detective quantum efficiency (DQE) (6–8), using the standard quality beam IEC RQA-M2 (9) (28 kV Mo-Mo, additional filtration: 2 mm, type 1199 Al).

Films were digitized using a high-resolution digitizer (Epson Expression 1680-Pro; Seiko Epson Corporation, Nagano, Japan) with an optical resolution of 1600×3200 dpi. A full characterization of the scanner

in terms of MTF and NPS was obtained, according to the procedure described (10). This characterization was used to correct results presented for the screen-film. The spatial resolution of the scanner was assessed using a test film pattern (Sine Patterns, Rochester, N.Y., USA). Noise characterization of the scanner was achieved using a set of optical gelatin filters (Kodak Wratten; Eastman Kodak Company, Rochester, N.Y., USA).

MTF quantifies image sharpness by measuring the signal transfer property as a function of spatial frequency. In this work, the presampling MTF was measured by using the slit technique. An oversampled line spread function (LSF) was obtained using a 10-μm tantalum slit. Exponential fitting of the oversampled LSF was performed, in order to reduce the effect of noise in the tails. The MTFs presented are the average of those obtained along the two orthogonal axes.

DQE describes how the signal-to-noise ratio is distributed across the system in relation to spatial frequency. DQE was measured at different exposures and was calculated using the following formula:

$$DQE(f) = \frac{\gamma^2 \cdot MTF^2(f)}{NNPS(f) \cdot q}$$

where NNPS is the normalized noise power spectrum, and q is the photon fluence determined by the half-value layer (HVL). Because the image pixel values were converted to exposure prior to calculation of the MTF and NPS, the system gain, γ, was unity. The HVL thicknesses (mm Al) were estimated from logarithmic interpolation of the measured exposure values. From tabulated data, we calculated the photon fluence at the average X-ray energy considered, and the number of photons per unit of area at the measured exposure was then calculated. More details about the procedures for performing the physical characterization are described in RIVETTI et al. (8). In view of the complexity of the analogue image digitization procedure, the DQE of the conventional system was calculated for an exposure of about 100 μGy, corresponding to an optical density of reference of 1.2 for the screen-film systems (11).

Contrast-detail analysis

To assess the contrast-detail characteristic, we used the CDMAM 3.4 phantom developed in Nijmegen (Artinis Medical Systems B.V., Arnhem, The Netherlands). This phantom permits determination of threshold contrast (object thickness) as a function of object diameter. The results are plotted as a contrast-detail curve, presenting the observed threshold contrast for a defined X-ray exposure as a function of object size. CDMAM consists of a matrix of squares (16 rows and 16 columns), each square containing two identical gold disks of known thickness and diameter. One disk is placed in the center and the second in a randomly chosen corner. The observer has to indicate the corner where the eccentric disk is located. The phantom covers a range of object sizes and thicknesses representing possible lesions in the breast. The object diameters range between 60 μm and 2 mm, whereas the thicknesses range between 0.03 and 2 μm of gold, resulting in a radiation contrast range of about 0.5–30% at standard mammography exposure conditions. Within a row, the disk thickness is constant with logarithmically varying diameter. The contrast-detail curve can be viewed as the "separation" limit between the two image conditions where details are visible or invisible.

SFM (standard dose) vs. CRM (standard dose). In this initial analysis, the phantom was exposed using both systems in accordance with the conditions specified by the manufacturer for analogue images, i.e., 28 kV (Mo-Mo), 40 mm of PMMA, anti-scatter grid, compression paddle off, and a dose calculated to ensure that the mean optical density of the analogue image would correspond to 1.2 plus fog (approximately 100 μGy at the detector). Even if this optical density value is lower than those recommended by some screening programs (e.g., the NHS Breast Screening Programme), other studies suggest that the optimum optical density can differ from that range and should be determined for each film-screen combination and processing condition (12). These authors found that the optimum optical density was 1.25 for a film-screen similar to the one used in the present paper. Four images were produced for each condition, and the results obtained are the average of the curves obtained from the lightbox readings of four skilled readers, repeated twice at least 7 days apart.

CRM (standard dose) vs. CRM (low dose). This second analysis aimed to quantify the reduction in perceptibility noted when the digital analysis obtained in the previous phase was compared with an equivalent obtained with a dose 35% lower. Various recent studies (13–15) have demonstrated that, with digital mammography units, it is feasible to reduce the dose within the range 30–40% (and in some cases up to 50%), with respect to screen-film systems. First, we intended to test if a reduction within that range was practicable on phantoms. After that, in the next section, we assessed whether the same reduction could be achievable on clinical images, without affecting the diagnostic accuracy. Since this comparison was between two digital images, the reading was made on the computer screen, and, in order to assist the operator in evaluation of the CDMAM image and reduce the statistical error in the evaluation process, a graphical user interface (GUI; Fig. 1) developed for

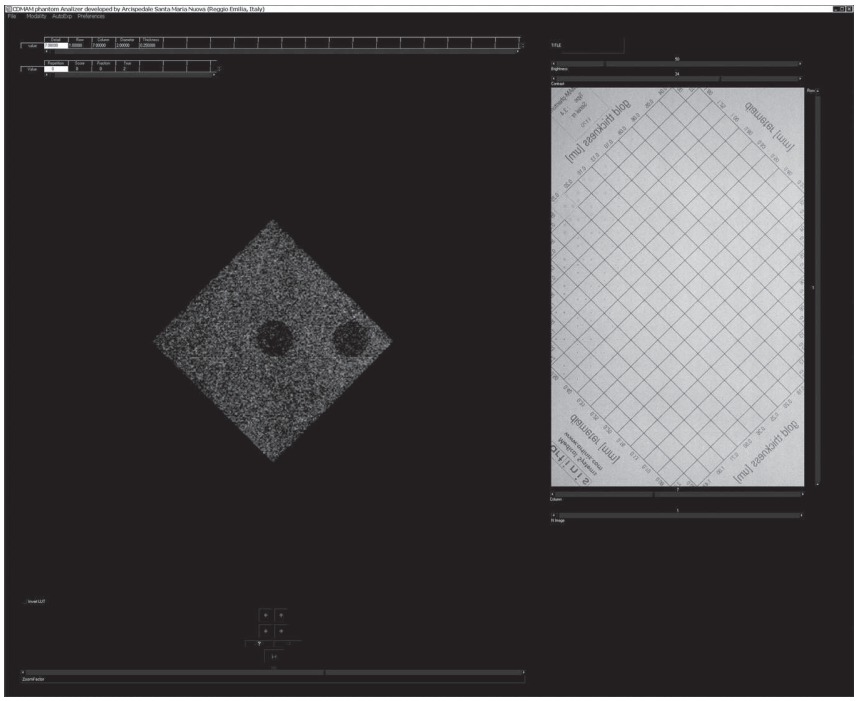

Fig. 1. The main panel of the program used for the contrast-detail analysis: on the right, the image of the phantom, and on the left, a single cell for preset zooming, brightness, and contrast. After each choice, the image is randomly rotated through an angle of 90, 180, or 270 degrees.

this specific purpose was used (8). The software allows reading and recording of the linearized image phantom files generated, while an operator chooses the vertex where he assumes the additional target is supposed to be by clicking on one of four keys. The software is freely available at URL: www.df.unibo.it/medphys.

Four experienced operators compared the two CRM system exposure conditions (four images per condition), the first (105 μGy) corresponding to the optimal exposure of the phantom for a mammographic screen-film system (standard dose), and the second (70 μGy) corresponding to a dose reduced by 35% ("low dose").

In the perceptibility "transition region," each target evaluation was repeated 20 times by each observer, in order to reduce the intra- and interoperator statistical error, and to define the contrast-detail curve we used the computation methodology proposed by SURYANARAYANAN et al. (16). In this case, the CDMAM images were evaluated by fixing display parameters such as zoom, brightness, and contrast to predefined values.

ROC analysis

Each CRM clinical image was interpreted in both soft copy (SC) and hard copy (HC), and both sets of HC images were viewed on a dedicated lightbox with a luminance of 4000 cd/m2. To avoid the reading order effect, the SFM and CRM images were interpreted in random order (fewer than 40 different images each session).

The ROC analysis was logged using RocKit software developed by Charles E. Metz at the Department of Radiology of the University of Chicago (17); the area under the ROC curve (AUC) was calculated to compare the systems. The statistical difference between the curves obtained was calculated by means of an analysis-of-variance (ANOVA) test.

The postprocessing algorithm settings were fixed at the same value for all the ROC analyses, at the following values: GA: 1.4; GC: T; GT: 1.40; GS: -0.08; MRB: C; MRT: P; MRE: 0.8; MDB: E; MDT: F; MDE: 0.8. These parameters define the gradation processing (rotation amount, rotation center, gradation type, and density shift, respectively), the spatial frequency processing, and the dynamic range control.

Results

Physical characterization

Figs. 2A and B show the results obtained from calculation of the MTF and DQE, respectively. While returning a lower MTF, due to the spread of the stimulating laser within the phosphor layer throughout the

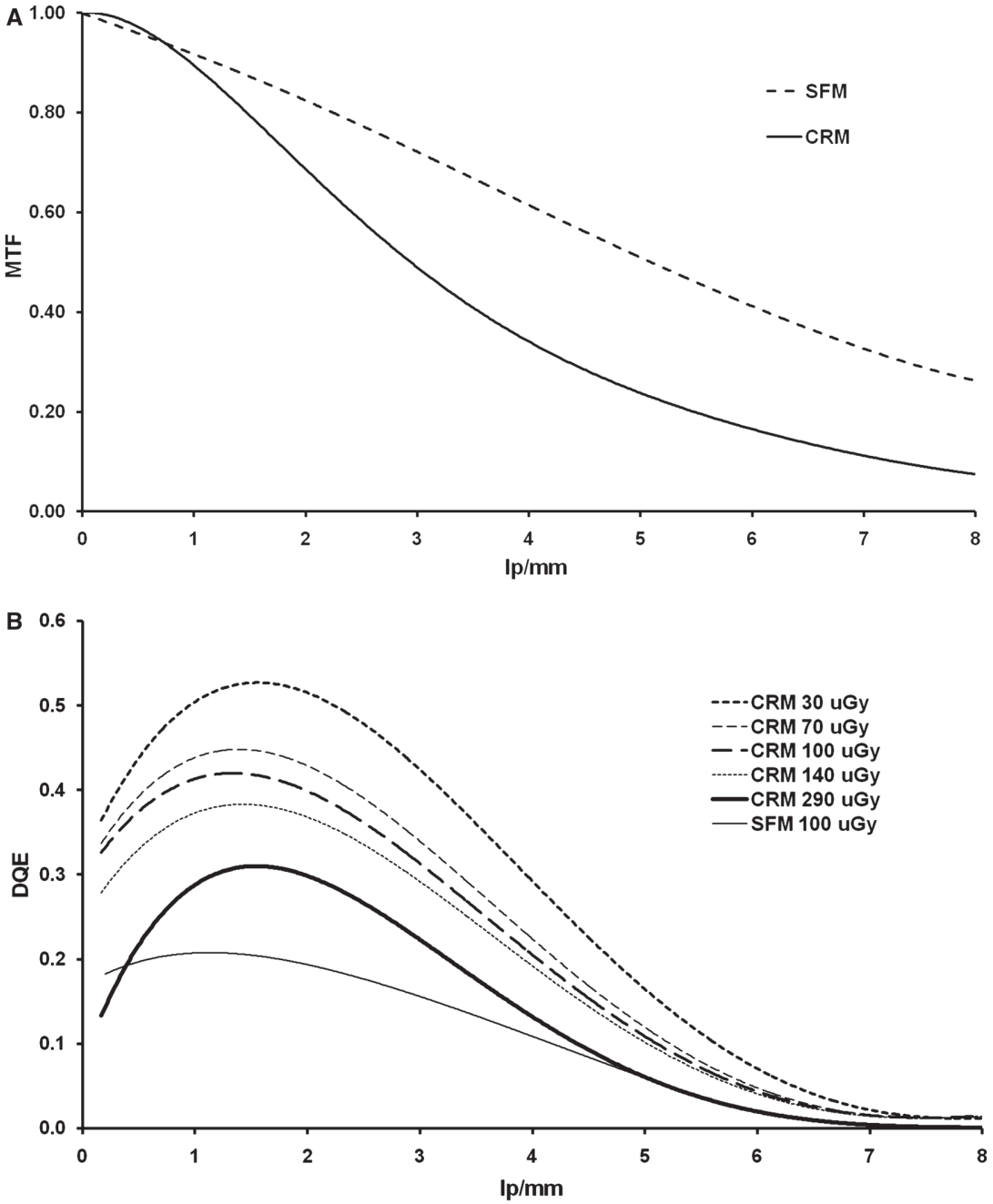

Fig. 2. A, MTF: SFM and CRM systems (28 kV Mo-Mo). B, DQE: SFM and CRM systems (28 kV Mo-Mo).

frequency range, the digital system always had a higher DQE. The DQE of the CRM system was found to decrease with increasing exposure, due to an increased relative contribution of CR system noise. It is likely that the granular structure of the storage phosphor contributed to increased noise with increasing exposure at all frequencies and that large area nonuniformity contributed significantly to decreasing DQE values at low frequency.

Contrast-detail analysis

SFM (standard dose) vs. CRM (standard dose). This analysis (Fig. 3) revealed that, with the same exposure

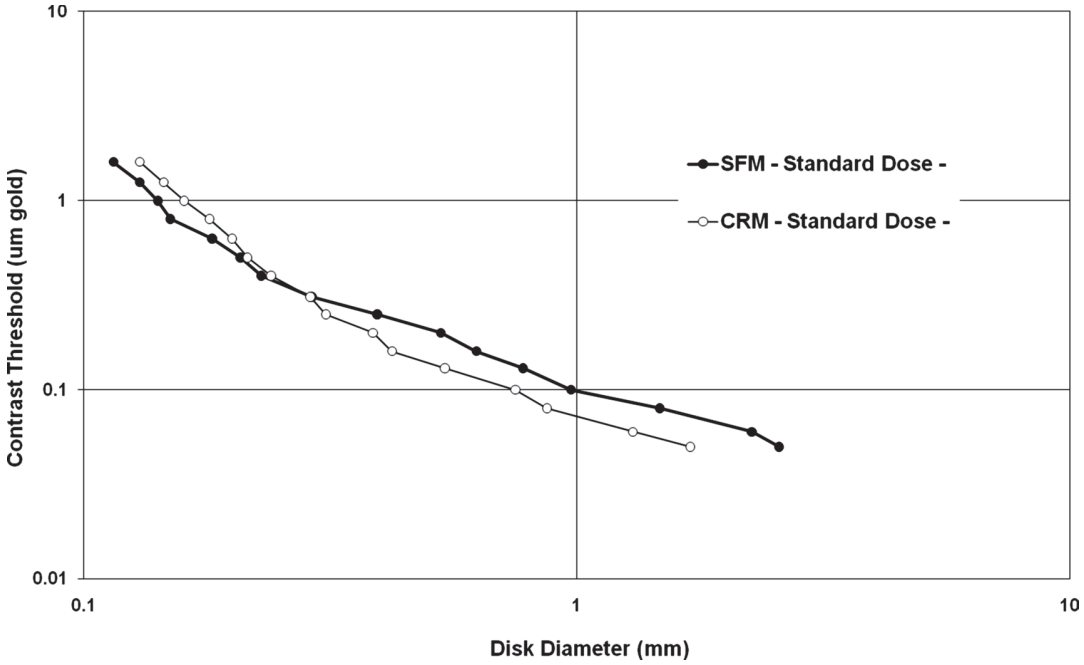

Fig. 3. Contrast-detail curves: SFM vs. CRM (standard dose).

conditions, the digital system always gave a better response for details larger than 150 μm in size. Conversely, the digital system gave a worse response for details smaller than 150 μm. These results agree very well with others published for comparing the same FUJIFILM CR system to similar screen-film combinations (18,19).

CRM (standard dose) vs. CRM (low dose). Fig. 4 shows the curves generated by the averages of the readings of four expert readers, who assessed the two sets of four images acquired with the two different detector exposures of 105 μGy (standard dose) and 70 μGy (low dose), respectively. As expected, the curve relating to the exposure of 70 μGy (lower performance) is higher, but there is no statistically significant difference (Mann-Whitney) compared to the curve for the standard dose.

ROC analysis

The distribution of the thicknesses of the compressed breasts for the investigated patients was basically Gaussian, with a mean of 4.3 cm and standard deviation of 1.2 cm. Fig. 5 illustrates the exposure conditions in terms of average glandular dose (AGD) (20, 21) for the SFM and the CRM systems, calculated by the X-ray source output. The average of the AGD distributions (SFM 2.22 mGy; CRM 1.44 mGy; Fig. 5A and B, respectively) reveals that the average dose used with the digital system was 35% lower than with the screen-film system.

The results of the ROC investigation of the two diagnostic systems are shown in Fig. 6, with a distinction between the hard-copy and soft-copy readings for the digital system.

The differences in the areas underneath the ROC curves (AUC) were not statistically significant (ANOVA, $P>0.05$); in other words, when CRM was used with a 35% reduction in dose, the curves showed that the diagnostic performance of the two systems was substantially equivalent.

Discussion

In conventional systems, the response function that defines the degree of blackening of the film in relation to the incident radiation on the detector depends mainly on the development conditions and the characteristics of the screen-film complex. These features intrinsically determine the doses of radiation needed to obtain the highest possible diagnostic content in the image produced. On the other hand, in digital systems, the user is able to obtain images of different appearance, and thus of different diagnostic content, within a broad range of administered doses, compared to film. Digital techniques offer significant advantages in terms of management, especially the postprocessing, archiving, and transfer of images.

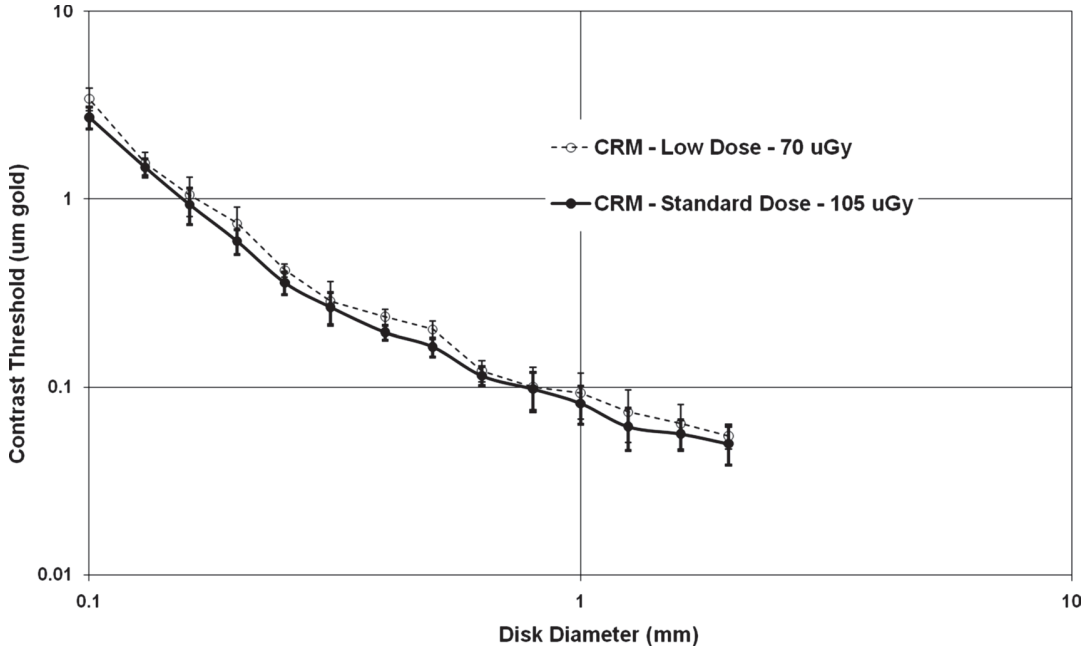

Fig. 4. Contrast-detail curves for the CRM system: standard dose vs. low dose.

This work aimed to perform a clinical comparison between a CRM unit and a conventional SFM system, first with the same exposure conditions and then with reduced dose to the patient. To this end, it was necessary to deepen our knowledge of the detector's intrinsic performance capabilities, and to obtain quantitative information concerning the optimal exposure condition.

The physical characterizations of the two systems were developed in terms of spatial resolution (MTF) and contrast resolution (DQE). Specifically, as in other studies (5,8), we found that the DQE of a CR system, other than being greater than the DQE of the conventional SFM system, has the property of returning decreasing values for increasing doses. Subsequently, the contrast-detail analyses were used for two main aims, firstly to verify that the perceptive performance of the CRM system (using the default postprocessing settings) is at least comparable to the SFM system in the same exposure condition, as also reported by other studies (22,23), and secondly to investigate the loss of perceptive performance linked to the reduction of the incident dose to the detector. It should be emphasized that, in the second contrast-detail analysis, the images produced with the digital system were interpreted without the aid of the display tools typical of this technology, i.e., zoom, brightness, and contrast, which tend to improve perceptive performance, especially for small-sized details (24). The idea behind keeping the window level fixed was to provide the same settings under all viewing conditions to all readers, without worrying too much about the absolute performance that can be gained. We did not focus our attention on obtaining the best absolute results in terms of visibility of details. Rather, we were more interested in the comparison between the contrast-detail results at the two dose levels considered.

In the clinical context, the ROC analysis showed that the areas under the ROC curves for CRM (both hard copy and soft copy) were found to be basically equivalent to the screen-film method in diagnostic terms (25). This confirms that an improved CR DQE, compared to the conventional system, could be used to reduce the dose administered, as reported in literature for other full-field digital mammography systems (15, 16, 26). Other authors (27, 28) have shown that the AEC can be calibrated for better use in CR systems. This optimization could further reduce the dose, by selecting harder X-ray spectra, with respect to the screen-film systems. It is worth noting that, in our case, with the CR system, we were able to obtain a comparable clinical image quality with a 35% dose reduction, without performing any specific optimization on the X-ray beam. Thus, in principle, a further reduction in dose could be achievable with the CR system if an appropriate calibration of the AEC is performed. Obviously, for a CRM system, matching with an AEC system is of great importance in clinical practice, and therefore such matching needs to be customized, according to the clinical situation.

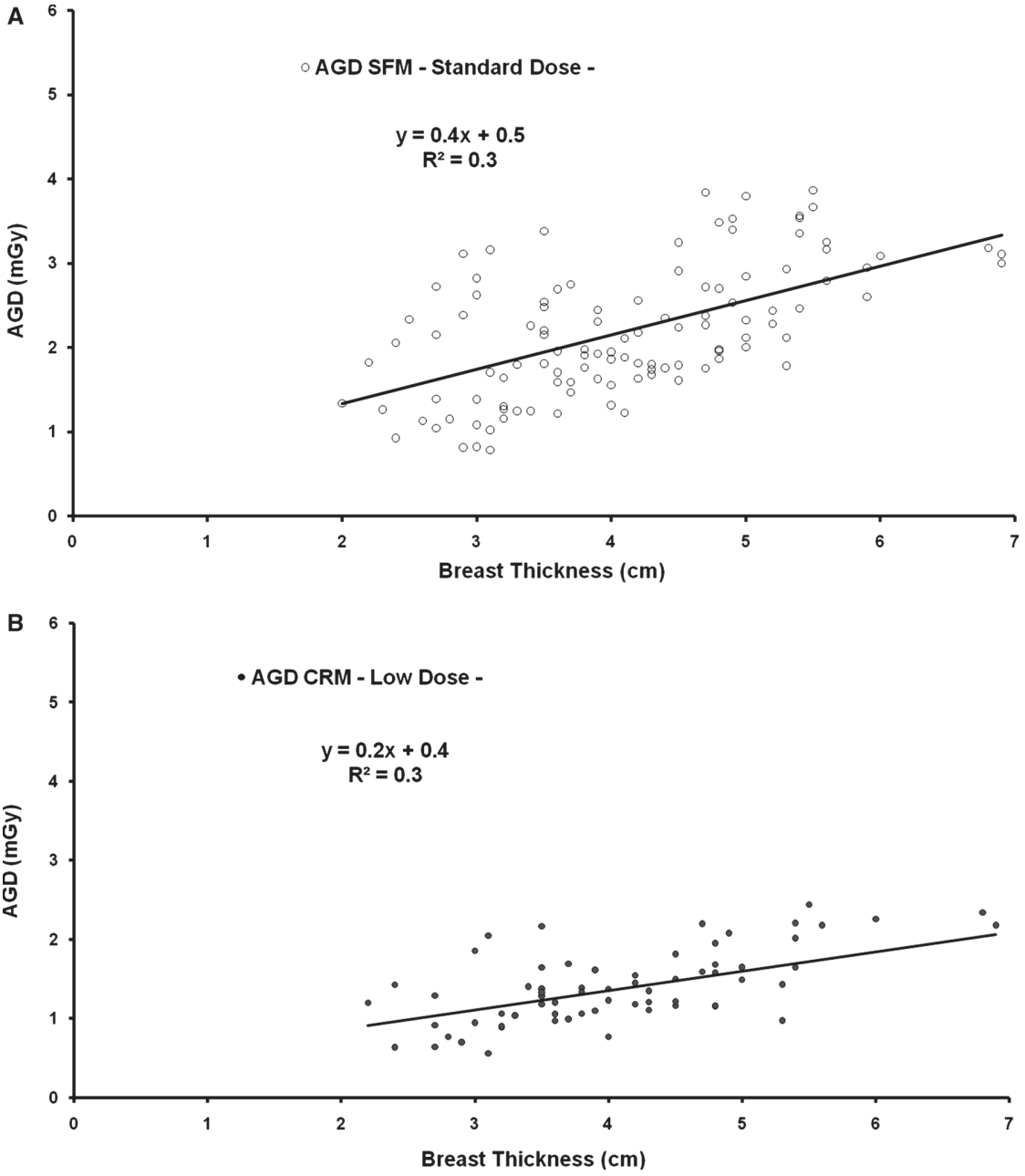

Fig. 5. A, Average glandular dose distribution vs. breast thickness, for the SFM system. B, Average glandular dose distribution vs. breast thickness, for the CRM system.

The results obtained reveal a reassuring compatibility between the phantom study and the ROC curves, therefore stressing the importance of preliminary studies for successful optimization of a digital system. In this work, all images were acquired on the same mammography unit. CR technology is fully compatible with conventional Bucky tables and allows the acquisition of almost identical images, since even the compression can remain fixed. This condition, not always achievable, offers the ideal situation for comparing both kinds of images.

A limitation of this study is that specific investigation could be required to establish whether the correlation between the phantom study and clinical evaluations continues to apply in breasts with a particular configuration. A comparative feature analysis study, using appropriately selected features, such as inhomogeneous background, could provide this specific information.

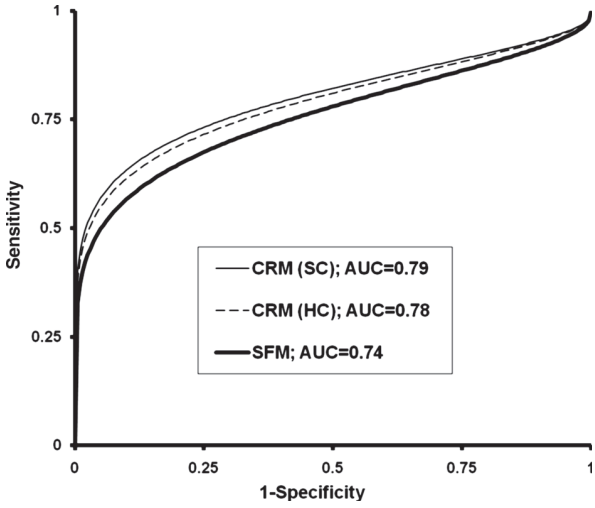

Fig. 6. ROC curves for the SFM and CRM systems. Also shown are the values of the area under the curves (AUC).

Another limitation of the presented study is that the number of patients enrolled was not very high. An investigation with more patients could help to improve the statistical significance of the diagnostic performance.

In conclusion, the comparison achieved in this work suggests that the use of the dual-side CRM system is a very good alternative to the screen-film system. In fact, the CRM is able to provide a diagnostic performance equivalent to SFM, with a 35% reduction in dose to patients.

Acknowledgments

The authors would like to thank Massimiliano Gerosa for his interest in the present work and for his helpful suggestions in postprocessing-algorithm development. “Authors are also grateful to the technicians of the Radiological Department - Policlinico of Modena, Italy, for their invaluable assistance in the clinical acquisitions.

References

1. Lewin JM, Hendrick RE, D’Orsi CJ, Isaacs MF. Comparison of full field digital mammography with screen–film mammography for cancer detection: results of 4,945 paired examinations. Radiology 2001;218:873–80.
2. Skaane P. Studies comparing screen-film mammography and full-field digital mammography in breast cancer screening: updated review. Acta Radiol 2009;50:3–14.
3. Monnin P, Gutierrez D, Bulling S, Lepori D, Valley JF, Verdun FR. A comparison of the performance of modern screen-film and digital mammography systems. Phys Med Biol 2005;50:2617–31.
4. Zaumlhringer M, Reineck S, Perniok A, Kruumlger K, Andermahr J, Rubbert A, et al. Digital amorphous silicon flat-panel detector radiography at different exposure doses versus mammography film: possibility of radiation dose reduction in detecting rheumatologic bone defects. Acta Radiol 2008;49:157–66.
5. Fetterly KA, Schueler BE. Performance evaluation of a dual side-read dedicated mammography computed radiography systems. Med Phys 2003;30:1843–54.
6. Borasi G, Nitrosi A, Ferrari P, Tassoni D. On site evaluation of three flat panel detectors for digital radiography. Med Phys 2003;30:1719–31.
7. Borasi G, Samei E, Bartolini M, Nitrosi A, Tassoni D. Contrast-detail analysis of three flat panel detectors for digital radiography. Med Phys 2006;33:1707–19.
8. Rivetti S, Lanconelli N, Campanini R, Bertolini M, Borasi G, Nitrosi A, et al. A comparison of different commercial FFDM units by means of physical characterization and contrast-detail analysis. Med Phys 2006;33:4199–209.
9. International Electrotechnical Commission. Medical diagnostic X-ray equipment – radiation conditions for use in the determination of characteristics. IEC-61267, Geneva, Switzerland, 2003.
10. Verdun FR, Pachoud M, Bergmann D, Buhr E. Assessment of radiographic screen-film systems: a comparison between the use of a microdensitometer and a drum film digitiser. Radiat Prot Dosimetry 2005;114:208–13.
11. Borasi G. Valutazione della qualità di sistemi radiografici schermo-pellicola: principi fisici e metodi di misura. Radiol Med 1990;32:807–14.
12. McParland BJ, Boyd MM, Al Yousef K. Optimizing optical density of a Kodak mammography film-screen combination with standard-cycle processing. Br J Radiol 1998;71:950–3.
13. Gennaro G, di Maggio C. Dose comparison between screen/film and full-field digital mammography. Eur Radiol 2006;16:2559–66.
14. Fischer U, Hermann KP, Baum F. Digital mammography: current state and future aspects. Eur Radiol 2006;16:38–44.
15. Svahn T, Hemdal B, Ruschin M, Chakraborty DP, Andersson I, Tingberg A, et al. Dose reduction and its influence on diagnostic accuracy and radiation risk in digital mammography: an observer performance study using an anthropomorphic breast phantom. Br J Radiol 2007;80:557–62.
16. Suryanarayanan S, Karellas A, Vedantham S, Ved H, Baker SP, D’Orsi CJ. Flat-panel digital mammography systems: contrast-detail comparison between screen-film radiographs and hard-copy images. Radiology 2002;225:801–7.
17. Metz CE. ROC methodology in radiologic imaging. Invest Radiol 1986;21:720–3.
18. Herman KP, Obenauer S, Zach-Enk A, Grabbe E. A new CR based system for high resolution mammography: experimental analysis of low contrast detectability. In: Peitgen HO, editor. Digital mammography: IWDM 2002 – 6th International Workshop on Digital Mammography; 2002 June 22–25; Bremen, Germany. Berlin: Springer; 2003. p. 111–3.
19. Van Engen RE, Veldkamp WJH, Oostveen LJ, Thijssen MAO, Karssemeijer N. Image quality of a dual side reading Fuji computed mammography system compared to the GE FFDM system and a film/screen mammography system. In: Peitgen HO, editor. Digital mammography: IWDM 2002 – 6th International Workshop on Digital Mammography; 2002 June 22–25; Bremen, Germany. Berlin: Springer; 2003. p. 155–7
20. Dance DR, Skinner CL, Young KC, Beckett JR. Additional factors for the estimation of mean glandular dose using UK mammography protocol. Phys Med Biol 2000;45:3225–40.

21. Van Engen R, Young KC, Bosmans H, Thijssen M. The European protocol for the quality control of the physical and technical aspects of mammography screening. In: European guidelines for breast cancer screening. Fourth edition. Luxembourg: European Commission; 2006.
22. Heddson B, Rönnow K, Olsson M, Miller D. Digital versus screen-film mammography: a retrospective comparison in a population-based screening program. Eur J Radiol 2007;64:419–25.
23. Bonardi R, Ambrogetti D, Ciatto S, Gentile E, Lazzari B, Mantellini P, et al. Conventional versus digital mammography in the analysis of screen-detected lesions with low positive predictive value. Eur J Radiol 2005;5:258–63.
24. Young KC, Cook JH, Oduko JM, Bosmans H. Comparison of software and human observers in reading images of the CDMAM test object to assess digital mammography systems. In: Flynn MJ, Hsieh J, editors. Medical imaging 2006: physics of medical imaging; 2006 Feb 11–16; San Diego, CA, USA. Proc. SPIE, Vol. 6142, 614206.
25. Obenauer S, Hermann KP, Schorn C, Fischer U, Grabbe E. Full-field digital mammography: dose-dependent detectability of breast lesions and microcalcinosis. Rofo. 2000;172:1052–6.
26. Hermann KP, Obenauer S, Marten K, Kehbel S, Fischer U, Grabbe E. Average glandular dose with amorphous silicon full-field digital mammography: clinical results. Rofo 2002;174:696–9.
27. Young KC, Oduko JM, Bosmans H, Nijs K, Martinez L. Optimal beam quality selection in digital mammography. Br J Radiol 2006;79:981–90.
28. Satoh K, Kuwabara T, Yasuda H, Arakawa S. Optimization of image quality and average glandular dose in CR mammography, In: Hsieh J, Flynn MJ, editors. Medical imaging 2007: physics of medical imaging; 2007 Feb 17–22; San Diego, CAUSA. Proc. SPIE, Vol. 6510, 65104H.